

ORIGINAL ARTICLE

CT Imaging of Cancer and Normal Cells with Gold Nanoparticles as Contrast Agent: An In-Vitro Study

Amirah Jamil¹, Moshi Geso², Wan Nordiana W Abd Rahman¹

¹ Medical Radiation Programme, School of Health Sciences, Universiti Sains Malaysia, 16150 Kubang Kerian, Kelantan, Malaysia

² Discipline of Medical Radiation, School of Health and Biomedical Sciences, RMIT University, Bundoora VIC 3083, Melbourne, Australia

ABSTRACT

Introduction: Computed tomography (CT) imaging has progressively developed from only structural imaging tool into hybrid diagnostic imaging such as PET-CT and SPECT to aid clinicians in diagnosis and treatment for cancer. Nowadays, researchers have found that CT might have a good prospect to become a molecular imaging modality. This research aim was to study the effects of gold nanoparticles (AuNPs) as contrast agent in computed tomography (CT) imaging. **Methods:** Samples of H₂O, hFOB, HeLa, and MCF-7 with and without AuNPs were scanned at 80, 100, 120, and 140 kVp to investigate the influence of tube potential settings towards CT enhancement in Hounsfield (HU) unit. Regions of interests (ROIs) were drawn and the CT values were compared. **Results:** The results show noticeable contrast enhancements of the samples incubated with AuNPs in CT images compared to the samples without AuNPs. hFOB, HeLa, and MCF-7 with AuNPs show contrast enhancement of 1.3 to 1.5 times greater than the cell lines samples without AuNPs. The outcomes also demonstrate that samples irradiated with 80 kVp yield improved CT values compared to other tube potential settings. **Conclusion:** The results obtained evidenced AuNPs have the potential to be a contrast agent for CT molecular imaging based on their ability in contrast enhancement.

Keywords: Contrast agent, Diagnostic imaging, Molecular imaging, Nanoparticles, Tomography

Corresponding Author:

Wan Nordiana W Abd Rahman, PhD

Email: wandiana@usm.my

Tel: +609-7677811

INTRODUCTION

Medical imaging has important role in overall cancer management as a diagnostic tool, for cancer staging, radiation treatment planning and evaluation of treatment efficiency. Computed tomography (CT) is one of the gold standard imaging modalities in clinical settings for cancer diagnosis and considered as structural imaging modality due to its ability to identify anatomical abnormalities and give out basic yet valuable information such as tumor position, size and the extent of spreading based on endogenous contrast. However, CT is not able to detect and can barely distinguish between benign and malignant mass in metastases progression that are less than 0.5 cm (1). CT also cannot distinguish between different soft tissues with almost similar densities, thus the need to use contrast agent was introduced for decades to improve not just the delineation of soft tissue structures with similar or identical contrast properties but it also provides better vascular contrast. After years of using commercial iodine-based contrast agent, research has

found that there are risks of side effects of radiographic contrast media ranging from mild forms such as rashes and itching, to severe reaction, for instance, contrast-induced nephropathy, delayed allergy reactions, anaphylactic reactions, and cutaneous reactions upon administration of this agent (2).

One of the ways to solve this limitation is by using gold nanoparticles (AuNPs) as contrast agent for CT. Recently there were a lot of conducted researches that found and proven that AuNPs have better properties which could enhance high quality contrast in CT image compared to commercial iodine-based contrast agent with less adverse effects and has low-risk safety profile in at least 24 organs (3). AuNPs also has the ability to act as dyes due to the surface plasmon resonance (SPR) and has distinctive features such as remarkable optical and electronic properties, high stability and biological compatibility, controllable morphology and size dispersion, and easy surface (4 - 8), plus functioning as biosensors of proteins and DNA that can be used for tumor cells imaging.

Since CT scan has low sensitivity in detecting very small mass, it might reduce the efficiency in detecting early-stage cancer. Lately, the development of new engineered

nanomaterials has been blooming and AuNPs is one of the intriguing metal nanoparticles that hold suitable properties as a contrast agent. This application of novel contrast agent might allow CT imaging to advance into molecular imaging modality.

MATERIALS AND METHODS

AuNPs preparation

The experiments were conducted using 1.9 nm AuroVist (Nanoprobes, NY, USA) and was diluted with Dulbecco’s Modified Eagles Medium (DMEM, Gibco, USA) to obtain a concentration of 10 mMol AuNPs solution and the AuNPs was further diluted until it reaches final concentration of 5 mMol using the following formula:

$$M_1V_1 = M_2V_2 \quad (1)$$

Where M_1 refers to molarity (moles/litres) of initial concentration of AuNPs solution, V_1 refers to volume of concentrated solution needed, M_2 refers to the molarity of diluted solution after more solvent has been added, and V_2 refers to volume of the diluted solution.

Cell culture (hFOB, HeLa, and MCF-7)

hFOB (human fetal osteoblast), HeLa (cervical cancer) and MCF-7 (human mammary carcinoma) cell lines were cultured in Dulbecco’s Modified Eagles Medium (DMEM) (Gibco, USA), supplemented with 10% fetal bovine serum (FBS) (Gibco, USA) and 1% penicillin-streptomycin (Gibco, USA). The cells were incubated under 37°C temperature, humidified with 5% CO₂ to grow. Phosphate Buffered Saline (PBS) (Gibco, UK) was used to wash out excess debris contained in culture flasks and rinse the remaining media during subculturing.

Routine passaging every 48 to 72 hours to subdivide the cells into fresh medium were done by detaching adherent cells with adequate 0.025% trypsin-EDTA (Gibco, USA). 24 hours before irradiation, all cell culture samples that have to be treated with AuNPs were transferred into 6-well plates using the same trypsinization method during subculturing. An amount of 1 x 10⁵ live cells/ml were suspended into each well and was treated with AuNPs for 24 hours, allowing the nanoparticles to attach to adherent cells. On the day of irradiation, the cell lines solution and H₂O with and without AuNPs were filled into 1.5 ml Eppendorf tubes.

Irradiation protocol

After the cells has been prepared, all samples including H₂O with and without AuNPs were arranged in Styrofoam block to hold the samples in place during irradiation as illustrated in Figure 1. Irradiation was done using CT scanner (Siemens Definition AS, Siemens Medical Solutions Inc., USA) at four different tube potential settings (80 kVp, 100 kVp, 120 kVp and 140 kVp) using head imaging protocol with slice thickness of 0.6 mm. Only axial plane images were obtained to get

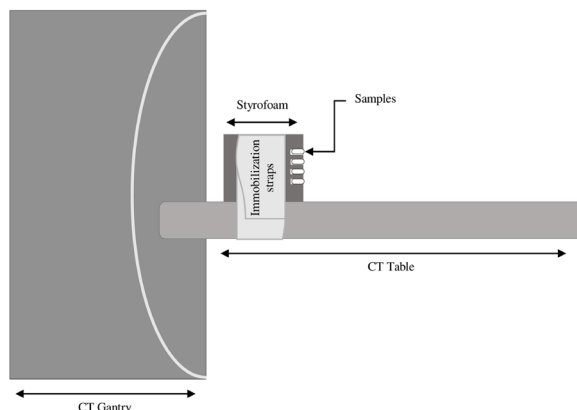


Figure 1: The set-up for CT irradiation. All samples were arranged inside a Styrofoam with the aid of immobilization device to avoid motion while scanning

an ample information on the HU value of each sample to indicate the CT enhancement. HU values were obtained by tracing the outline of regions of interests (ROIs) from each sample, excluding the background Styrofoam and the wall of Eppendorf tubes.

RESULTS

The mean CT attenuation of H₂O, hFOB, HeLa and MCF-7 with and without AuNPs at different tube potential settings are summarized in Table I. A bar graph and line graphs are plotted based on the results in Table I are shown in Figure 2 and Figure 3 (a), (b), (c) and (d).

Table I: Mean CT Attenuation (HU)

kVp	H ₂ O		hFOB		HeLa		MCF-7	
	With AuNPs	Without AuNPs	With AuNPs	Without AuNPs	With AuNPs	Without AuNPs	With AuNPs	Without AuNPs
80	106.3 ± 0.96	5.8 ± 0.76	29.9 ± 1.37	22.5 ± 0.62	22.7 ± 0.9	14.3 ± 1.51	2.1 ± 3.18	14.7 ± 0.76
	94.9 ± 0.76	9.1 ± 0.64	23.3 ± 0.83	17.3 ± 2.19	21 ± 0.97	14.2 ± 1.56	21.4 ± 2.55	14.4 ± 0.55
120	85.9 ± 1.01	7.5 ± 0.38	18.5 ± 0.98	10.7 ± 0.4	17.8 ± 0.57	9.7 ± 1.21	20.2 ± 1.08	8.7 ± 0.36
	75.1 ± 0.6	7.5 ± 0.32	13.5 ± 0.95	10.8 ± 0.17	12.6 ± 0.67	7.8 ± 0.5	14 ± 0.67	9.4 ± 1.02

The table shows the mean CT attenuation of different types of samples with different tube potential settings. Abbreviations: kVp, tube potential (kilovoltage peak); hFOB, human foetal osteoblast cell; HeLa, cervical cancer cell; MCF-7, human mammary adenocarcinoma cell.

Improved CT attenuation is evident between the sample with and without AuNPs especially in H₂O, with at least 10 times greater enhancement after AuNPs is introduced. hFOB as normal cell lines yield at least 1.3 times greater CT attenuation with AuNPs, followed by HeLa cell with 1.4 times increase in CT attenuation and MCF-7 which possess the highest contrast enhancement of 1.5 times greater than MCF-7 without AuNPs. The trends of the results for kVp against CT attenuation could be observed in Figure 3 (a), (b), (c) and (d). Contrast

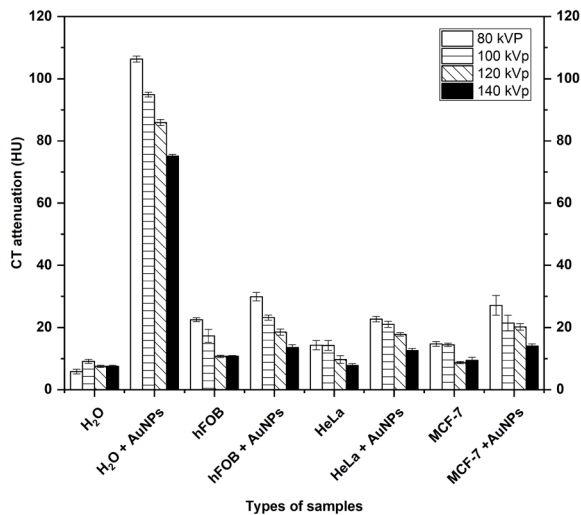
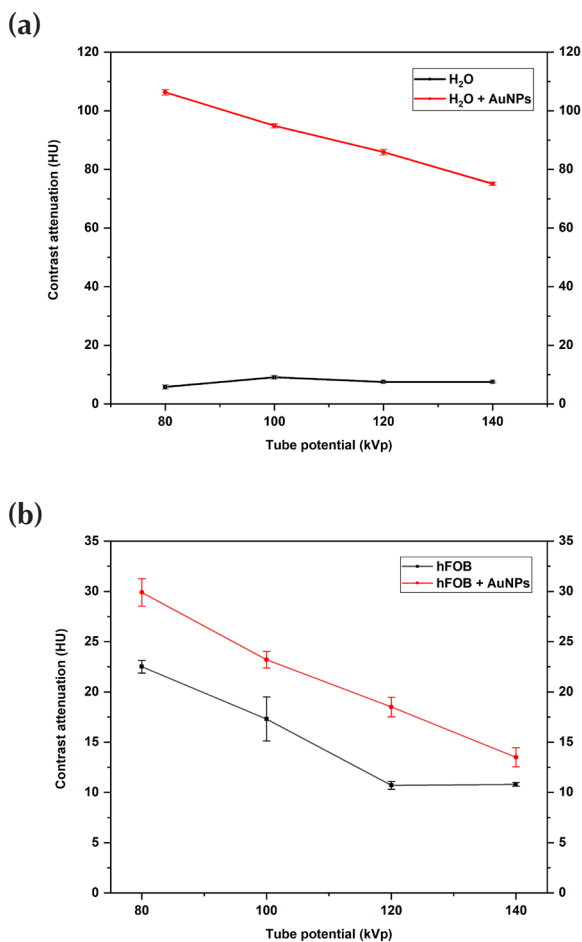


Figure 2: CT attenuation of H₂O, hFOB, HeLa and MCF-7 (with and without AuNPs) using 80, 100, 120 and 140 kVp tube potentials.

enhancement of H₂O with AuNPs steadily decreases as the kVp increases, while H₂O without AuNPs slightly increases in CT attenuation at 100 kVp and decreases slightly in CT attenuation at 120 and 140 kVp.



Other apparent results between H₂O as control and all types of cells used in this study is that the values for H₂O with AuNPs marked an impressive difference compared with H₂O without AuNPs as well as cell lines with and without AuNPs that show significant differences. Comparing the attenuation difference of H₂O and cells with AuNPs, the increase of 10 times enhancement compared to 1.3 - 1.5 times of that in cells necessitates a justification.

The result for hFOB with and without AuNPs gradually decreases with increased kVp, except the marked similarity in HU of hFOB without AuNPs at 120 kVp and 140 kVp. Meanwhile, HeLa and MCF-7 with AuNPs also have similar trends of decreasing HU values with increased kVp. For HeLa and MCF-7 without AuNPs, a noticeable drop of HU values could be observed at 100 and 120 kVp. Additionally, the level of CT enhancement between MCF-7 with AuNPs is different than that of HeLa will also be discussed in this study.

DISCUSSION

The definition of CT attenuation value is defined as the material radiodensity expressed in HU, with distilled

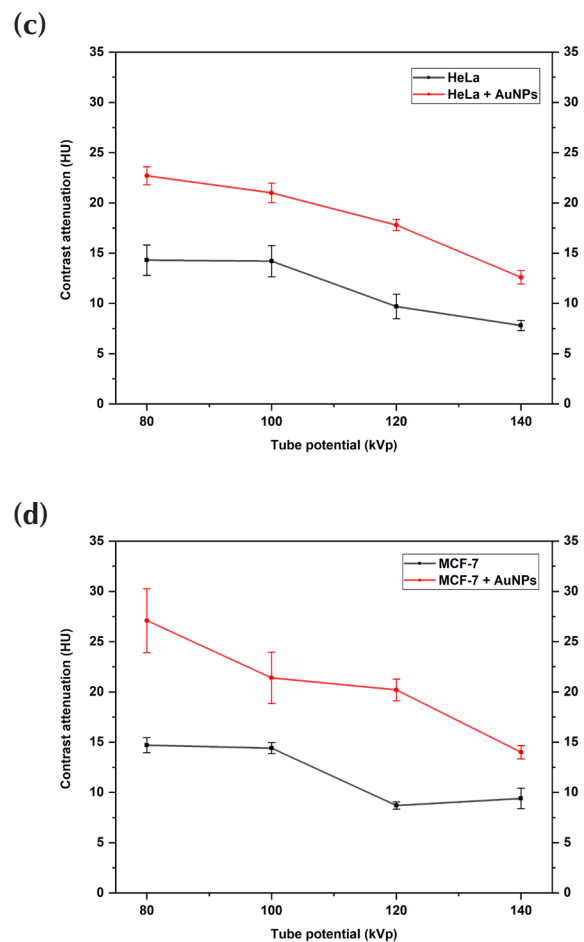


Figure 3: CT attenuation (HU) of (a) H₂O with and without AuNPs, (b) hFOB with and without AuNPs, (c) HeLa with and without AuNPs and (d) MCF-7 with and without AuNPs at different tube potential settings.

water of standard temperature and pressure theoretically holds HU of 0, whereas air holds HU of -1000 (9). Based on our study, the values obtained from H₂O without AuNPs are more than 0, which might be due to difference in temperature or pressure of the distilled water used in this research. In previous research, it has been reported that CT HU value accuracy may be influenced by patient size, shape, variation of position in the scanner, scatter, spectral energy, convolution kernel, reconstruction artifacts and beam hardening or whether an anthropomorphic body phantom is used (10). Since we used 1.5 ml Eppendorf tubes in this work, slight variability in HU value of H₂O was expected.

Based on the observation in Figure 2, the comparison between the HU of H₂O with AuNPs and cells with AuNPs marked huge difference. This is attributable to the method of this study which requires the cultured cells to be rinsed with PBS to remove excess debris and the extracellular- attached AuNPs. The process of nanoparticles internalization at cellular level is called pinocytosis (11). In other words, the outcome of the measured HU values of cells after introduction of AuNPs are the measurement of the intracellular AuNPs. Relatively, AuNPs inside the cells are still able to produce significant enhancement of HU value when compared to the H₂O sample with AuNPs.

AuNPs possess 2.7 times higher in mass attenuation compared to iodine due to its high density and higher atomic number (12). However, the size, shape and concentration of AuNPs have been reported to influence cellular uptake and the contrast enhancement in CT imaging (13 - 15). Some research discovered that AuNPs smaller than 60 nm resulted in greater attenuation than the larger size (16 - 17). In a study by Dou et al. stated otherwise. From their observation, using various AuNPs sizes from 3.9 nm to 41.1 nm, larger AuNPs produced higher contrast than the smaller AuNPs (18). Different particles shapes and concentration might be the cause of conflicting results in previous studies. Our study used a single size of AuNPs (1.9 nm), which increases the nanoparticles uptake in the cells thus increasing the CT attenuation between the samples.

X-ray penetration ability is determined by the energy applied to the subject of interest. In an acquisition, the differences between anatomical structures are highly influenced by the penetration power, which could be adjusted by modifying the kVp before exposing the subject to radiation. The alteration of kVp in turn changing the radiation dose, exposure, and contrast (19). In this study, it is apparent that higher energy imposed on the samples degrades the contrast enhancement. The HU decrease with the utilization of higher kVp is due to lower contrast caused by higher scattered Compton photons when using higher kVp. This signifies that lower tube potential used in CT will result in higher CT attenuation. In a study using commercial iodine-based

contrast agent and tantalum as new contrast agent, the optimal kVp for excellent contrast and dose efficiency for both materials are 80 kVp and 100-120 kVp, respectively (20).

The cancer cells, MCF-7 and HeLa with AuNPs, shows different levels enhancement despite seeded with the same number of cells in 6-well plates before irradiation. Proven by previous study, HeLa grew slower than MCF-7 based on the cellular growth curve (21). Since the results show that HU value is dependent on the cell uptake of AuNPs, lesser number of cells will anticipate produce lower HU value. Due to the prospect of HeLa having lower HU value due to its slow growth compared to MCF-7 despite similar number of cells (1 × 10⁵ live cells/ml), further study is needed to investigate the effects of the cell's number and its relationship with the degree of CT enhancement.

CONCLUSION

This study proved the feasibility of AuNPs as potential novel contrast agent for CT molecular imaging based on the enhancement in HU values between cell lines with and without AuNPs. The results indicate 1.3 times of enhancement in HU values were observed in hFOB, 1.4 times enhancement in HeLa and 1.5 times enhancement in MCF-7 cell lines. The highest contrast enhancement of CT images was seen at the lowest kVp settings (80 kVp) while the lowest contrast enhancement was at higher kVp settings (120 and 140 kVp) for all types of samples. This agreed to the previous studies that higher tube potential settings produce higher chance of scatter radiation which could lower the contrast enhancement in CT radiographic images. The AuNPs has high prospect as contrast agent in CT molecular imaging due to higher contrast enhancement in different types of cells.

ACKNOWLEDGEMENT

We thank the staff members of Hospital Universiti Sains Malaysia (HUSM) for their assistance in our work. This study is supported by Ministry of Higher Education Fundamental Research Grant Scheme (FRGS/1/2020/STG07/USM/02/2).

REFERENCES

1. Popovtzer R, Agrawal A, Kotov NA, Popovtzer A, Balter J, Carey TE, et al. Targeted gold nanoparticles enable molecular CT imaging of cancer. *Nano Lett.* 2008;8(12):4593–4596.
2. Andreucci M, Solomon R, Tasanarong A. Side Effects of Radiographic Contrast Media: Pathogenesis, Risk Factors, and Prevention. *Bio Res Int.* 2014;2014:1–12.
3. Kojima C, Umeda Y, Ogawa M, Harada A, Magata Y, Kono K. X-ray computed tomography

- contrast agents prepared by seeded growth of gold nanoparticles in PEGylated dendrimer. *Nanotechnology*. 2010;21(24),1–5.
4. Huang X, Jain PK, El-Sayed IH, El-Sayed MA. Gold nanoparticles: Interesting optical properties and recent applications in cancer diagnostics and therapy. *Nanomedicine*. 2007;2(5):681–693.
 5. Kircher MF, Willmann JK. Molecular Body Imaging: MR Imaging, CT, and US. Part I. Principles. *Radiology*. 2012;263(3):633–643.
 6. Pan D, Williams TA, Senpan A, Allen JS, Scott MJ, Gaffney PJ, et al. Detecting vascular biosignatures with a colloidal, radio-opaque polymeric nanoparticle. *J. Am. Chem. Soc.* 2009;131(42):15522–15527.
 7. Li J, Chaudhary A, Chmura SJ, Pelizzari C, Rajh T, Wietholt C, et al. A novel functional CT contrast agent for molecular imaging of cancer. *Phys Med Biol*. 2010;55(15):4389–4397.
 8. Chen Z, Wang Y, Lin Y, Zhang J, Yang F, Zhou Q, et al. Advance of Molecular Imaging Technology and Targeted Imaging Agent in Imaging and Therapy. *Bio Res Int*. 2014;2014:1–12.
 9. Seishima R, Okabayashi K, Hasegawa H, Tsuruta M, Hoshino H, Yamada T, et al. Computed tomography attenuation values of ascites are helpful to predict perforation site. *World J Gastroenterol*. 2015;21(5):1573–1579.
 10. Lamba R, McGahan JP, Corwin MT, Li CS, Tran T, Seibert JA, et al. CT Hounsfield Numbers of Soft Tissues on Unenhanced Abdominal CT scans: Variability Between Two Different Manufacturers' MDCT Scanners. *AJR Am J Roentgenol*. 2014;203(5):1013–1020.
 11. Foroozandeh P, Aziz AA. Insight into Cellular Uptake and Intracellular Trafficking of Nanoparticles. *Nanoscale Res Lett*. 2018;13(1):339.
 12. Hainfeld JF, Dilmanian FA, Slatkin DN, Smilowitz HM. *J Pharm Pharmacol*. 2008 Aug; 60(8):977-85.
 13. Chithrani, B. D., Ghazani, A. A. & Chan, W. C. W. Determining the size and shape dependence of gold nanoparticle uptake into mammalian cells. *Nano Letters* 6(4), 662–668 (2006).
 14. Hajfathalian, M. et al. Wulff in a cage gold nanoparticle as contrast agents for computed tomography and photoacoustic imaging. *Nanoscale* 10(39), 18749–18757 (2018).
 15. Chhour, P. et al. Effect of gold nanoparticle size and coating on labeling monocytes for CT tracking. *Bioconjugate Chem*. 28(1), 260–269 (2017).
 16. Khademi, S. et al. Evaluation of size, morphology, concentration, and surface effect of gold nanoparticles on X-ray attenuation in computed tomography. *Phys. Med.* 45, 127–133 (2018).
 17. Xu, C., Tung, G. A. & Sun, S. Size and concentration effect of gold nanoparticles on X-ray attenuation as measured on computed tomography. *Chem. Mater*. 20(13), 4167–4169 (2008).
 18. Dou, Y. et al. Size-tuning ionization to optimize gold nanoparticles for simultaneous enhanced CT imaging and radiotherapy. *ACS Nano* 10(2), 2536–2548 (2016).
 19. Tonnessen BH, Pounds L. Radiation physics. *J Vasc Surg*. 2011 Jan;53(1 Suppl):6S-8S.
 20. Rui X, Jin Y, FitzGerald PF, Alessio A, Kinahan P, Man BDe. (2014). Optimal kVp Selection for Contrast CT Imaging Based on a Projection-domain Method. *Conf Proc Int Conf Image Form Xray Comput Tomogr*. 2014; 2014:173–177.
 21. Song K, Xu P, Meng Y, Geng F, Li J, Li Z, et al. Smart gold nanoparticles enhance killing effect on cancer cells. *Int J Oncol*. 2013;42(2):597-608.